

Mixture of Experts in Image Classification: What’s the Sweet Spot?

Mathurin Videau^{1,2}, Alessandro Leite¹, Marc Schoenauer¹, Olivier Teytaud²

¹TAU, Inria Saclay,
²Meta AI, FAIR Labs

Abstract

Mixture-of-Experts (MoE) models have shown promising potential for parameter-efficient scaling across various domains. However, the implementation in computer vision remains limited, and often requires large-scale datasets comprising billions of samples. In this study, we investigate the integration of MoE within computer vision models and explore various MoE configurations on open datasets. When introducing MoE layers in image classification, the best results are obtained for models with a moderate number of activated parameters per sample. However, such improvements gradually vanish when the number of parameters per sample increases.

Introduction

Recent advancements in machine learning, particularly in the domains of natural language processing (NLP) (Vaswani et al. 2017; Kenton and Toutanova 2019) and computer vision (Dosovitskiy et al. 2020), have been primarily driven by scaling up model size, computational budgets, and training data. While these large-scale models demonstrate impressive performance, they are often expensive to train and consume considerable energy resources (Strubell, Ganesh, and McCallum 2019). As a result, the research community has been increasingly interested in exploring more efficient training and serving paradigms. One such promising solution is the use of sparse expert models, with Mixture-of-Experts (MoE) (Shazeer et al. 2017; Lepikhin et al. 2020). MoE models introduce sparsity by partitioning the set of parameters into multiple parallel sub-models, referred to as “experts”. During training and inference, the gating part of the models routes input examples to specific expert(s), ensuring that each example only interacts with a subset of the network parameters. As the computational cost is, partially, correlated with the number of parameters activated for a given sample rather than the total number of parameters, this approach facilitates the scaling-up of the model, while keeping computational costs under control, making it an attractive option for a wide range of applications.

Despite their success in various domains (Hihn and Braun 2021; Costa-jussà et al. 2022; Zoph et al. 2022; Fedus, Zoph, and Shazeer 2022), the application of MoE models in computer vision remains limited, and it often requires very large datasets (Riquelme et al. 2021; Mustafa et al. 2022; Komatsuzaki et al. 2022) to be competitive against state-of-the-art

approaches. In this work, we first focus on leveraging the potential of MoE models for computer vision on ImageNet-1k and ImageNet-21k (Russakovsky et al. 2015). We study the efficiency of integrating MoE within two renowned architectures, ConvNext (Liu et al. 2022) and Vision Transformer (ViT) (Touvron, Cord, and Jégou 2022). We conduct a series of experiments considering various architecture configurations. Likewise, we investigate the impact of various components, including the number of experts and their sizes, the gate design, and the layer positions, among others. Our experimental findings indicate that the optimal design is contingent on the specific network architecture, and that consistently situating the MoE layer within the final two even blocks invariably yields substantial improvements for moderate model size. However when scaling up the approach to large models and large datasets, close to the state of the art, the benefits of using MoE for image classification seem to gradually vanish.

Related Works

The Mixture-of-Experts (MoE) model, introduced by Jacobs et al. (1991), partitions complex tasks into hopefully simpler sub-tasks handled by expert models, whose predictions are combined to produce the final output. This framework has been successfully integrated into various neural network architectures, particularly transformers for NLP tasks (Shazeer et al. 2017). Given this success in NLP, interest has burgeoned in applying MoE to the diverse and complex realm of computer vision.

The transformative potential of MoE architectures is underscored by their successful integration across various domains, with the Vision Transformer (ViT) being a prime example. Riquelme et al. (2021) introduced V-MoE, an MoE-augmented ViT model, for image classification tasks on a massive dataset containing hundreds of millions of examples. They showed that V-MoE does not only match the performance of prior state-of-the-art architectures, but it also requires half the computational resources during inference. Lou et al. (2021) presented a sparse MoE MLP model based on the MLP-Mixer architecture (Tolstikhin et al. 2021). While the MLP-Mixer architecture does not display performance accuracy, the MoE-enhanced version surpassed its dense counterpart in experiments on ImageNet and CIFAR. Hwang et al. (2022) demonstrated the effec-

tiveness of SwinV2-MoE, a MoE-based model built upon Swin Transformer V2 architecture. They reported superior accuracy in downstream computer vision tasks. A similar work (Puigcerver et al. 2023) introduced a soft MoE mechanism, demonstrating improved performance and training speed compared to classical MoE on billion-scale datasets.

Sparingly Activated MoE

Based on conditional computations, MoE aims at activating specific parts of the model depending on the input. The core idea is to assign experts to different regions of the input space, thereby increasing the model capacity by augmenting the number of parameters without incurring significant computational overhead (Jacobs et al. 1991).

According to Shazeer et al. (2017), an MoE includes a router G and a set of experts E . The router learns a sparse assignment between the input and the experts, while the experts process the inputs like standard neural network modules do. Let x be the input, and let $(E_i)_{i \in [1, N]}$ be the N experts of the MoE layer. Following (Shazeer et al. 2017), the output of this MoE layer is given by:

$$\sum_{i \in \text{Top}_k(x)} G(x)_i \cdot E_i(x),$$

where G is a $\text{conv}1 \times 1$ gate employing a softmax function, and $G(x)_i$ is its i^{th} output. To promote sparsity in the MoE layer, the number of participating experts is restricted to $k < N$ for each input: $\text{Top}_k(x)$ contains the indices of the k highest $G(x)_i$. Note that involving $k > 1$ experts increases the computational cost compared to the sparse ($k = 1$) counterpart. We tested several gate designs, but none of them clearly outperformed the simple $\text{conv}1 \times 1$ gate (Table 10 in Appendix).

However, enforcing this MoE design is insufficient to yield an effective MoE. To exploit compute capacity optimally, we encourage uniform usage of each expert by using a load balancing auxiliary loss proposed in (Shazeer et al. 2017), which promotes balanced expert assignments and equal importance of experts (For more details, see Section 4 of Shazeer et al. (2017)). We also use Batch Prioritized Routing (BPR) introduced by Riquelme et al. (2021).

Vision Transformer

The Vision Transformer (ViT) (Dosovitskiy et al. 2020) represents a paradigm shift in computer vision. It moves away from traditional convolution-based architectures in favour of the Transformer’s attention mechanism, initially pioneered for natural language processing tasks (Vaswani et al. 2017). In the ViT model, an image is segmented into fixed-size and non-overlapping patches. These patches are linearly embedded into vectors and then passed through a series of Transformer blocks. Each Transformer block is predominantly made up of two main components: a multi-head self-attention mechanism and a multi-layer perceptron (MLP). Within the context of ViT, the MLP ratio (denoted `mlp_ratio` in the following) refers to the ratio of the hidden dimensions of the MLP to the embedding dimensions. This ratio is pivotal, as it determines the capacity and computational cost

of the MLP component. We replace some predefined MLP block by a MoE, as depicted in Figure 1a. Each MoE operates at the patch level: the experts are spatially distributed.

ConvNext

ConvNext (Liu et al. 2022) has modernized the classical convolutional neural networks (CNN) design by incorporating insights from Vision Transformers (ViT). The central component of the ConvNext architecture is a block containing a 7×7 depth-wise convolution followed by a 1×1 convolutional layer (Figure 1b-left). This block is replicated across four stages, each with decreasing resolution. In this work, we replace some predefined ConvNext block, namely the multilayer perceptron, with a MoE block, and introduce a skip connection, as illustrated in Figure 1b-right. Consequently, each expert becomes a fully convolutional block operating at the feature map level, resulting in spatially distributed experts. Hence, this design does not only increase the network capacity, but it also allows each expert to specialize in specific spatial locations, and engages multiple experts per image.

Experiments on ImageNet

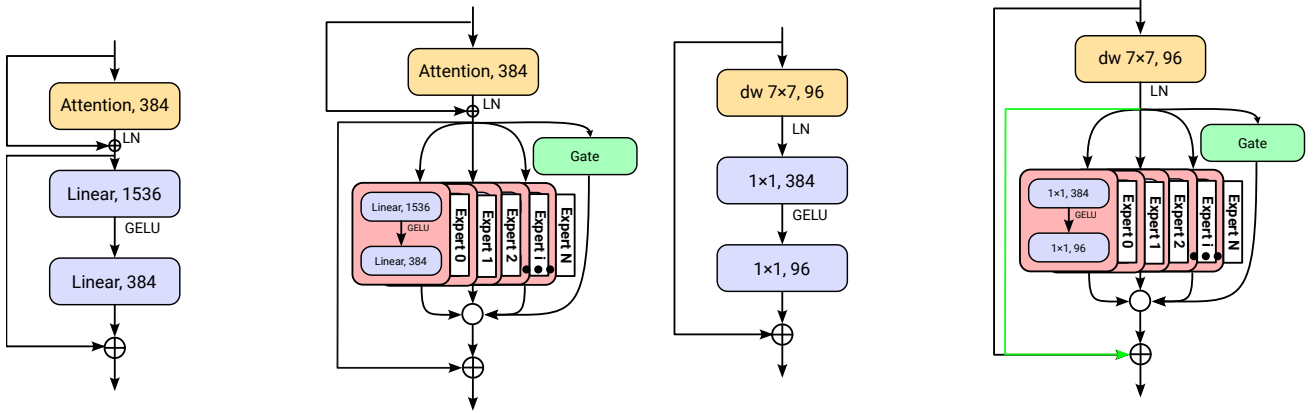
This section presents the results obtained by the architectures described above (that incorporate MoE into the ConvNext and ViT architectures), trained on ImageNet-1k or pre-trained on ImageNet-21k datasets. It includes the experimental setup, the results on the ImageNet-1k validation set, and the impact of various MoE configurations.

Experimental setup

All the results presented in this section rely on MoE models trained on the ImageNet datasets. Even though the context is different because of the changes of network structures presented in the previous sections, we set the training hyperparameters similar to (Touvron, Cord, and Jégou 2022) for ViT and (Liu et al. 2022) for ConvNext (a grid search looking for better settings did not bring significant improvement). Furthermore, when working with the ImageNet-1k dataset, we use a strong data-augmentation pipeline, including Mixup (Zhang et al. 2018), Cutmix (Yun et al. 2019), RandAugment (Cubuk et al. 2020), and Random Erasing (Zhong et al. 2020), over 300 epochs. Likewise, we utilize drop path, weight decay, and expert-specific weight decay as regularization strategies. However, for the pre-training phase on ImageNet-21k, we exclude Mixup and Random Erasing from the data augmentation pipeline because they did not improve results (as also reported in (Touvron, Cord, and Jégou 2022; Tu et al. 2022)). We pre-train the model for 90 epochs, adhering to the original ConvNext approach (Liu et al. 2022) and, consistently with Liu et al. (2022) and Touvron, Cord, and Jégou (2022), the final results of ImageNet-1k are obtained through fine-tuning for 30 epochs for ConvNext and 50 for ViT. Comprehensive details of all the hyperparameters are provided in Table 12 in the appendix.

Base results on ImageNet

Table 1 presents the results obtained on ImageNet-1k validation set by a model that has been entirely trained on



(a) **Left:** ViT base block. Right: Our modified MoE ViT block. LN: Layer normalization. GELU: Gaussian Error Linear Units.

(b) **Left:** ConvNext original base block. Right: The modified MoE ConvNext block. The green link represents the added skip connection. DW: Depth-wise. LN: Layer normalization.

Figure 1: Vision Transformer and ConvNext architectures.

ImageNet-1k, for isotropic architecture (e.g., ViT, ConvNext *iso.*) and a hierarchical architecture, namely ConvNext. We see some significant improvements in accuracy compared to the “no-MoE” results for small model size, especially for anisotropic models.

Table 2 presents the results of models that are pre-trained on ImageNet-21k, and tested on the same ImageNet-1k validation set than above. Here, MoE does bring some improvement for moderate numbers of activations per sample. However, this improvement decreases for large numbers of activations per sample. Figure 8 illustrates more examples.

Sensitivity with respect to design choices

This section presents different sensitivity studies that investigate the specifics of the design choices of the MoE layers. We explore the impact of the position of these layers inside the architecture, the effect of varying the number of experts, and finally, we assess the necessary design changes when transitioning from ImageNet-1k to ImageNet-21k dataset.

Impact of the position of MoE layers Table 3 displays the effects of various placements of MoE layers, comparing the following configurations: (a) **Every 2:** a MoE layer replaces every second layer; (b) **Stage:** a MoE layer replaces the final layer of each stage, resulting in four MoE layers throughout the network for ConvNext; (c) **Last 2:** a MoE layer replaces the final layer of each of the last two stages; (d) **Last 3:** Same as “Last 2”, but with an additional MoE layer inserted in the middle of stage 3.

As shown in Table 3, “Last 2” strategy is the most robust choice: it performs well across all architectures. On the opposite, “Every 2” performs worst for ConvNext architecture, and best for ViT. Consequently, in the following, all experiments use “Last 2” for ConvNext and “Every 2” for ViT.

Influence of the number of experts Table 4 presents the performance of ConvNext and ViT architectures on ImageNet-1K training with the “Last 2” strategy MoE layers. It provides a comprehensive view of how the number of

experts influences the size (parameter count) of the models, and their Top-1 accuracy on this dataset.

The experimental results suggest that four experts yield the best performance for ConvNext, while eight experts are optimal for ViT. This is showcased by the Top-1 accuracy rates, which are consistent at 82.1% for ConvNext with four experts, and reach a peak of 80.5% for ViT with eight experts. However, we note that increasing the number of experts to 16 has a detrimental effect on both architectures. Specifically, for ConvNext, the top-1 accuracy slightly drops to 81.7%, and for ViT, the performance plateaus at 80.2%. These findings highlight that while MoE layers can enhance model performance, there is a delicate trade-off to be struck in terms of the number of experts. Exceeding the optimal number can lead to suboptimal results, negating the potential benefits of the MoE integration. Furthermore, in our detailed analysis, we explore the interplay between the number and the size of each expert. Our investigation revealed that, for isotropic networks such as ViT and ConvNext *iso.*, reducing the size of experts adversely affects performance, while for ConvNext, it has no significant impact. Moreover, during the course of our experiments, we observed that while the Top-1 configuration was superior for ConvNext, the Top-2, for ViT configuration was comparable or even better than the ConvNext Top-1 configuration, leading us to employ Top-1 for ConvNext and Top-2 for ViT.

Results on ImageNet-21k Tables 7 and 8 present the results of models trained on ImageNet-21k, reporting ImageNet-1k accuracy after fine-tuning. We analyse the effect of MoE layer positioning, expert size (Table 7), and expert count (Table 8). The results demonstrate that, when large volumes of data are accessible, a greater number of experts can be effectively deployed. Notably, the use of sixteen experts, which was sub-optimal for ImageNet-1K, does not negatively affect performance on ImageNet-21k. This suggests that increasing the number of experts together with the volume of data could lead to valuable enhancements.

Architecture	#Params ($\times 10^6$)	Per sample #Params _{act}	FLOPs	Throughput (im/s)	IN-1K Accuracy
ConvNeXt-T (Liu et al. 2022)	28.6	28.6	4.5G	814	82.1
ConvNeXt-T-4 Last 2 Top 1	34.5	25.6	4.2G	768	82.1
ConvNeXt-S (Liu et al. 2022)	50	50	8.7G	466	83.1
ConvNeXt-S-4 Last 2 Top 1	56.1	47.3	8.5G	442	83.1
ConvNeXt-B (Liu et al. 2022)	88.6	88.6	15.4G	299	83.8
ConvNeXt-B-4 Last 2 Top 1	99.1	83.4	15.0G	289	83.5
ConvNeXt-S (<i>iso.</i>)	22.3	22.3	4.3G	1100	79.7
ConvNeXt-S-8 (<i>iso.</i>) Last 2 Top 1	38.9	22.3	4.3G	1031	80.3
ConvNeXt-B (<i>iso.</i>)	82.4	82.4	16.9G	336	82.0
ConvNeXt-B-8 (<i>iso.</i>) Last 2 Top 1	115.4	82.4	16.9G	303	81.6
ViT-S	22.0	22.0	4.6G	1083	79.8
ViT-S-8 Last 2 Top 2	38.6	25.0	5.3G	892	80.5
ViT-S-8 Every 2 Top 2	71.7	33.1	6.9G	724	80.7
ViT-B	86.6	86.6	17.5G	329	82.8
ViT-B-8 Every 2 Top 2	284.9	129.9	26.3G	227	82.5

Table 1: Accuracy for different ImageNet-1K trained models and the MoE strategies “Every 2” and “Last 2” (see text). “Top k ” correspond to the number of experts involved. Throughput is measured on V100 GPUs, following (Touvron et al. 2021). For ImageNet-1k, non-isotropic ConvNext models feature an mlp_ratio of 2, which contributes to their improved flops-per-sample efficiency compared to their dense counterparts.

In terms of MoE layer configuration, our data showed no performance improvements with the addition of more layers, and the “every 2” strategy again yielded the poorest results for ConvNext based architecture.

Discussion

Hierarchical vs isotropic models

First, one can note that the best MoE designs typically apply experts only to the last layers. ViT operates at the same resolution at each layer after the input images have been cut into patches. This isotropic design implies that MoE is applied at layers which are not particularly large. On the other hand, with hierarchical models such as ConvNext, applying MoE to the last layers considerably increases model size. Indeed, as presented in Table 8, employing eight experts doubles the size of the network in spite of using only two layers of MoE.

Positions and numbers of MoE layers

There are two prevalent strategies in the literature concerning the position of MoE layer: “Every 2” and “Last 2”. In the context of hierarchical architectures such as ConvNext, the “Every 2” strategy dramatically increases the number of weights while simultaneously yielding inferior results. However, for ViT “Last 2” and “Every 2” are two viable strategies. This is inline with the results of V-MoE (Riquelme et al. 2021) on large-scale datasets. Overall, our results confirm that “Last 2” is a solid starting point, as it consistently yields positive outcomes across all tested architectures. However, it may not always be the optimal choice for every architecture. For instance, in the case of ViT, “Every 2” demonstrates better results. Regarding the number of experts, we noted that model performance quickly saturates

with the number of experts, as reproduced in Table 8 (more details on Figure 5).

Evaluating MoE in image classification

With the ImageNet benchmark increasingly reaching saturation, the focus in contemporary computer vision models has shifted towards computational efficiency and scaling prowess. An essential question arises: *Does the MoE model enhance this aspect in image classification?*

Our experiments with ImageNet reveal an intriguing insight. While integrating MoE into models like ConvNext and ViT does enhance performance, this improvement tends to plateau in models exceeding 100M parameters. This observation aligns with existing literature, as evidenced by results presented in Figure 2 (See Table 14 and Figure 8). One can observe that as the base dense network increases, the performance disparity between MoE and its dense counterpart decreases.

Exploring this further in large-scale datasets, such as JFT 3 billion (Zhai et al. 2022), reveals similar findings. For instance, the vision transformer model SoViT, with 400M parameters (Alabdulmohsin et al. 2023), exhibits comparable performance to the 15B V-MoE (Riquelme et al. 2021) when both use ViT-based architectures. Similarly, when considering the JFT-3B dataset (Zhai et al. 2022), the 5.6B LiMoE-H model (Mustafa et al. 2022) and Coca-Large (Yu et al. 2022) lead to analogous results when evaluated on a per-sample parameter basis.

To summarize, while the MoE model does not appear to redefine the state-of-the-art when matched against dense models on both ImageNet and billion-scale datasets, its real strength emerges in enhancing smaller models. By integrating MoE, these compact models can achieve better perfor-

Architecture	#Params ($\times 10^6$)	Per sample #Params _{act}	FLOPs	IN-1K Accuracy	Linear prob Accuracy	0-shot Accuracy
ConvNeXt-T (Liu et al. 2022)	28.6	28.6	4.5G	82.9	81.8	44.3
ConvNeXt-T-8 Last 2 Top 1	70.0	28.7	4.5G	83.5	82.3	44.6
ConvNeXt-S (Liu et al. 2022)	50.3	50.3	8.7G	84.6	83.2	45.2
ConvNeXt-S-8 Last 2 Top 1	91.6	50.3	8.7G	84.9	83.6	45.3
ConvNeXt-B (Liu et al. 2022)	88.6	88.6	15.4G	85.8	84.9	45.8
ConvNeXt-B-8 Last 2 Top 1	162.0	88.6	15.4G	85.7	84.8	45.9
ViT-S	22.0	22.0	4.6G	82.6	81.7	44.2
ViT-S-8 Every 2 Top 2	71.7	33.1	6.9G	83.0	81.9	44.7
ViT-B	86.6	86.6	17.5G	85.2	84.0	45.7
ViT-B-8 Every 2 Top 2	284.9	129.9	26.3G	85.2	84.0	45.6

Table 2: Accuracy for ImageNet-21K pre-trained models and different adaptations with ImageNet-1K: *IN-1K* is standard fine-tuning, *Linear prob* is the training of a linear layer for the output probability layer (everything else being frozen), and *0-shot* is the direct application of the pre-trained model to ImageNet-1K. “Every 2” and “Last 2” are the corresponding MoE strategies (see text). “Top k ” corresponds to the number of experts involved.

Architecture	MoE	# Params		FLOPs	IN-1K
		$\times 10^6$	Sample		
ConvNext-T	no MoE	28.6	28.6	4.5G	82.1
ConvNext-T-8	every 2	54.3	17.0	3.8G	81.8
	stage	47.4	25.5	4.0G	82.1
	last 3	49.9	25.0	4.1G	82.1
	last 2	46.3	25.6	4.2G	82.1
ConvNeXt-S (<i>iso.</i>)	no moe	22.3	22.3	8.7G	79.7
ConvNeXt-S-8 (<i>iso.</i>)	every 2	96.7	22.3	8.7G	79.6
	last 2	38.9	22.3	8.7G	80.3
ViT-S	no MoE	22.0	22.0	4.2G	79.9
ViT-S-8	every 2	71.7	33.1	5.3G	80.7
	last 2	38.6	25.0	6.9G	80.5

Table 3: Comparative results for different positions of MoE layers: ImageNet-1k training on ConvNext-T and ViT-S, all employing 8 experts.

mance, pushing their capabilities closer to the forefront of current benchmarks. Yet, it is essential to acknowledge that, in the broader context, MoE might not drive significant advancements in the overall state-of-the-art. This nuanced perspective is further enforced in the appendix, with the data showcased in Table 14.

Robustness Evaluation

We evaluated MoE models, trained or fine-tuned on ImageNet-1k, against a range of robustness benchmark datasets, such as ImageNet-A (IMA) (Hendrycks et al. 2021b), ImageNet-R (IMR) (Hendrycks et al. 2021a), ImageNet-Sketch (IMSK) (Wang et al. 2019), and ImageNet V2 (IMV2) (Recht et al. 2019), the latter being used as a measure of overfitting. Table 9 reports Top-1 accuracy for all datasets.

Table 9 shows that MoE models underperform their dense counterparts on ImageNet-1k. These results seem to contradict the ones reported by Li et al. (2022) in which MoE mod-

Architecture	# experts	#Params ($\times 10^6$)	Per samples #Params _{act}	IN-1K Top 1 acc.
ConvNext-T	no MoE	28.6	28.6	82.1
ConvNext-T	4	54.3	25.5	82.1
	8	47.4	25.5	82.1
	16	46.3	25.5	81.7
ViT-S	no MoE	22.0	22.0	79.9
ViT-S	4	29.1	25.0	79.8
	8	38.6	25.0	80.5
	16	57.5	25.0	80.2

Table 4: Comparative results for different numbers of experts. ImageNet-1k training using the “Last 2” strategy.

MoE strategy	#Params ($\times 10^6$)	Per samples #Params _{act}	FLOPs	IN-1K Top 1 acc.
no MoE	28.6	28.6	4.5G	82.9
every 2	97.5	28.6	4.5G	82.9
stage	78.2	28.6	4.5G	83.5
last 3	70.0	28.6	4.5G	83.5
last 2	70.0	28.6	4.5G	83.5
last 2	46.3	25.6	4.2G	83.4
mlp_ratio 2				

Table 5: ImageNet-21k training on ConvNext-T employing 8 experts and an MLP ratio of 4 unless specified explicitly.

els appear as natural domain generalizers. We note that MoE models are better for the robustness metric, they were actually already better on ImageNet-1k. So, these results actually emphasize the success of MoE when the model is sufficiently small for being improved by a MoE, as discussed in the section “Evaluating MoE in Image Classification”: the domain generalization holds only in the regime in which MoE improves the base results.

Model Inspection

The objective of this section is to scrutinize the routing component of the model. We will present the top expert for each

# experts	#Params ($\times 10^6$)	Per samples #Params _{act}	FLOPs	IN-1K Top 1 acc.
no MoE	28.6	28.6	4.5G	82.9
8	54.3	28.6	4.5G	83.5
16	117.1	28.6	4.5G	83.6
32	211.6	28.6	4.5G	83.4

Table 6: ImageNet-21k training on ConvNext-T: comparison between various numbers of experts, with a MLP ratio of 4.

MoE strategy	#Params ($\times 10^6$)	Per samples #Params _{act}	FLOPs	IN-1K Top 1 acc.
no MoE	28.6	28.6	4.5G	82.9
every 2	97.5	28.6	4.5G	82.9
stage	78.2	28.6	4.5G	83.5
last 3	70.0	28.6	4.5G	83.5
last 2	70.0	28.6	4.5G	83.5
last 2				
mlp_ratio 2	46.3	25.6	4.2G	83.4

Table 7: ImageNet-21k training on ConvNext-T employing 8 experts and an MLP ratio of 4 unless specified explicitly.

# experts	#Params ($\times 10^6$)	Per samples #Params _{act}	FLOPs	IN-1K Top 1 acc.
no MoE	28.6	28.6	4.5G	82.9
8	54.3	28.6	4.5G	83.5
16	117.1	28.6	4.5G	83.6
32	211.6	28.6	4.5G	83.4

Table 8: ImageNet-21k training on ConvNext-T: comparison between various numbers of experts, with a MLP ratio of 4.

routing layer. Note that when considering the top-2 configuration, we only report, for this visualization, the top-1 of these two experts.

Visual Inspection. Figure 3 in appendix, provides a visualization of the portions of images that are assigned to the different experts. This reveals that some experts specialize in specific elements of an image, such as animals, buildings, or objects. This trend is especially apparent when considering the top-1 MoE, but the distinction becomes less clear with the top-2 MoE. In both instances, the clusters formed by each expert are challenging to interpret, and the spatial locations of each expert tend to lack clarity and can be quite ambiguous.

Number of experts involved per image. We quantified the average number of experts contributing to processing an image. In the initial layers, the majority of experts are typically engaged for each image. With fewer than eight experts, most are utilized, even in deeper layers. For instance, in the ViT model with eight experts, an average of seven experts contributed per image, while in the ConvNext model, they are six. As we increase the number of available experts per MoE layer, the number of contributing experts per image also rises. For example, in ConvNext with 16 experts, an average of 10.5 experts are involved, and with 32 experts, this number increases to 15.8. This suggests that each ex-

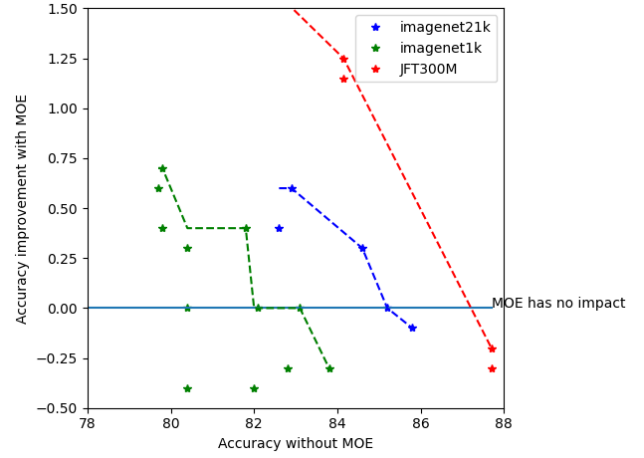


Figure 2: Improvement obtained thanks to MoE (y-axis) vs accuracy without MoE (x-axis), for different pretraining sizes and specifically for image classification. The more accurate the model, the lower the impact. The larger the pre-training, the greater the impact. For each pretraining size, a dashed line shows for each accuracy without MoE the maximum improvement obtained for at least this accuracy. Results are extracted from Tables 1, 2 and 14 (in Appendix).

pert is likely focused on a limited number of image patches. This observation is confirmed by the cumulative distribution function (CDF) of each expert per image, displayed in the appendix (see Figure 7 in the Appendix).

Correlation Between Experts and Labels. Figure 4 (top) in the Appendix presents the correlation between the number of expert occurrence and individual classes in ImageNet-1k. The class IDs in ImageNet-1k are organized in such a way that adjacent classes often share similar attributes. For instance, class IDs ranging from 151 to 268 are all dedicated to different dog breeds. From Figure 4, we note that the occurrences in the first three MoE layers do not match the ImageNet-1k classes, with most experts appearing uniformly across different classes. However, in the last three MoE layers, there is a noticeable trend of more experts aligning with specific ImageNet-1k classes. This distinction is especially pronounced between experts focusing on animals (classes up to ID 397, such as experts 0 and 6 in Figure 4-(e)) and those centred on objects (classes beyond ID 397, like experts 1 and 5 in Figure 4-(e)). As the number of experts increases, this class-specific alignment still holds, though it remains challenging to clearly define the roles of these experts since they often span several scattered classes rather than forming tight, contiguous groups that would fit each class, as illustrated in Figure 6 in the appendix.

Expert Similarity. In order to quantify the similarity between experts, we use a method derived from the Jaccard index. For each image, we tally the occurrences c_i of each expert E_i . The similarity between two experts, E_i and E_j , is defined as $S_{ij} = \frac{|E_i \cap E_j|}{|E_i \cup E_j|} = \frac{\sum^{E_i \cap E_j} c_i + c_j - |c_i - c_j|}{\sum^{E_i \cup E_j} c_i + c_j}$, where $E_i \cap E_j$ represents the images where both E_i and E_j appear

Model	IN-1K	IMV2	IMA	IMR	IMSK
Imagenet1k trained					
ConvNext-T	82.1	70.8	24.2	47.2	33.8
ConvNext-T-4	82.1	71.0	23.8	46.2	32.7
ConvNext-S	83.1	72.5	31.3	49.6	37.0
ConvNext-S-4	83.1	72.2	30.2	49.0	37.3
ConvNext-B	83.8	73.4	36.7	51.3	38.2
ConvNext-B-4	83.5	72.8	33.9	48.6	36.6
ViT-S	79.9	68.8	19.8	43.4	29.7
ViT-S-8	80.7	70.1	21.1	43.9	30.9
ViT-B	82.8	72.1	32.4	51.2	36.9
ViT-B-8	82.5	71.5	32.0	46.6	35.2
ConvNext-S (<i>iso.</i>)	79.7	68.6	13.0	46.4	34.0
ConvNext-S-8 (<i>iso.</i>)	80.3	68.8	13.5	46.6	34.4
ConvNext-B (<i>iso.</i>)	82.0	71.1	21.2	50.0	38.1
ConvNext-B-8 (<i>iso.</i>)	81.6	70.6	19.1	48.5	35.7
Imagenet21k pretrained					
ConvNext-T	82.9	72.4	36.2	51.1	38.5
ConvNext-T-8	83.5	72.8	32.6	51.3	40.8
ConvNext-S	84.6	74.7	44.8	57.5	43.6
ConvNext-S-8	84.9	75.5	44.4	55.7	45.5
ConvNext-B	85.8	76.0	54.6	62.0	48.8
ConvNext-B-8	85.7	76.3	51.8	59.6	48.4
ViT-S	82.6	72.6	38.9	50.8	39.0
ViT-S-8	83.0	72.7	35.3	51.0	39.4
ViT-B	85.2	76.1	56.0	61.5	46.9
ViT-B-8	85.2	75.4	48.1	59.3	45.9

Table 9: Robustness of MoE w.r.t. to domain change, for two different pretrainings both fine-tuned on ImageNet-1k: Top-1 accuracies on various datasets.

together, while $E_i \cup E_j$ refers to all images where either E_i or E_j is present at least once. The absolute value term $|c_i - c_j|$ acts as a corrective factor to account for scenarios where one expert may be deployed for a minimal number of patches while the other is utilized for the majority, indicating a lack of synergy between the two experts. In the bottom panel of Figure 4, we observe a distinct pattern in the utilization of experts across the stages of the MoE. In the initial layers, there is a prevalent co-occurrence of multiple experts, which highlights a concentration on local image features across all the images. Conversely, as we analyse deeper into the network, the frequency of expert co-occurrence diminishes. This shift indicates a transition in focus from local image elements to more semantically rich aspects, with individual experts concentrating on specific semantic attributes unique to certain images.

Are experts well partitioned, clustered?

Firstly, for a general task such as ImageNet-1k, there is no clear, natural decomposition into experts, making it difficult to precisely assess if one expert decomposition is better than another, aside from comparing final accuracy. This comparison, however, provides limited insight into the quality of the experts. The literature (Chen et al. 2023; Mittal, Bengio, and Lajoie 2022; Mohammed, Liu, and Raffel 2022) suggests that, without explicit enforcement, MoE models struggle to separate tasks or find natural clusters beneath them.

For instance, when a task separation was explicitly incorporated into the loss, there was a marked improvement in both accuracy and the ease with which experts could be pruned for specific tasks (Chen et al. 2023). Similarly, Mittal, Bengio, and Lajoie (2022) found that the enforced decomposition resulted in substantial gains, while the absence of such enforcement left the model unable to discover optimal partitions.

Consequently, we make three observations on ImageNet. (a) As the number of experts increases, there is a corresponding rise in the number of experts actively involved. Even with 32 experts, almost half of the experts are used per image in the last MoE layers. This seems counter-intuitive, since ImageNet is centred around objects, it should plateau at some point, at least for deep layers. Instead, experts are not well aligned with classes and spread widely, as depicted in Figure 4. (b) An analysis of the cumulative distribution function (CDF) of experts’ engagement (Figure 7 in the Appendix) reveals a prevalent trend where most experts are assigned to less than 20 patches of an image, equating to less than 10% of the total image area, 50% of the time. Moreover, these patches are not necessarily contiguous. (c) When we look at visualization of each expert like in Figure 3, we observe a concentration of experts in the image for MoE layers near the output. The interpretation of each expert’s role becomes challenging, and each expert does not seem to adhere closely to each object or to each part of the object location.

Conclusion

Implementing Mixture-of-Experts (MoE) models for computer vision tasks remains an open and challenging task. Our experimental findings indicate that using MoE in computer vision, particularly for large models, does not substantially surpass the current state-of-the-art in accuracy, robustness, domain generalization, or per-sample complexity. This observation applies to both convolutional networks and vision transformers. These results highlight a contrast between text processing and computer vision applications of MoE. While, in the text domain tasks, MoE models benefit from adding weighted components, enhancing knowledge storage within the model, in computer vision tasks, they predominantly hinge on extrapolation and feature extraction, where MoE models seem to offer limited advantages. Interestingly, we observe the most notable improvements in smaller-scale models, especially in image classification tasks, where the number of activated parameters per sample is low. In these cases, MoE layers provided moderate enhancements, suggesting that the effectiveness of MoE models in computer vision may be context- and scale-dependent. For instance, MoE models show potential benefits in scenarios with fewer activations per sample, in contrast with dense (non-MoE) models counterparts.

References

Alabdulmohsin, I.; Zhai, X.; Kolesnikov, A.; and Beyer, L. 2023. Getting ViT in Shape: Scaling Laws for Compute-Optimal Model Design. *arXiv:2305.13035*.

- Chen, Z.; Deng, Y.; Wu, Y.; Gu, Q.; and Li, Y. 2022. Towards understanding mixture of experts in deep learning. *arXiv:2208.02813*.
- Chen, Z.; Shen, Y.; Ding, M.; Chen, Z.; Zhao, H.; Learned-Miller, E. G.; and Gan, C. 2023. Mod-Squad: Designing Mixtures of Experts As Modular Multi-Task Learners. In *IEEE/CVF Conference on Computer Vision and Pattern Recognition*, 11828–11837.
- Chi, Z.; Dong, L.; Huang, S.; Dai, D.; Ma, S.; Patra, B.; Singhal, S.; Bajaj, P.; Song, X.; Mao, X.-L.; et al. 2022. On the representation collapse of sparse mixture of experts. *Advances in Neural Information Processing Systems*, 35: 34600–34613.
- Costa-jussà, M. R.; Cross, J.; Çelebi, O.; Elbayad, M.; Heafield, K.; Heffernan, K.; Kalbassi, E.; Lam, J.; Licht, D.; Maillard, J.; et al. 2022. No language left behind: Scaling human-centered machine translation. *arXiv:2207.04672*.
- Cubuk, E. D.; Zoph, B.; Shlens, J.; and Le, Q. V. 2020. Randaugment: Practical automated data augmentation with a reduced search space. In *IEEE/CVF Conference on Computer Vision and Pattern Recognition Workshops*, 702–703.
- Dosovitskiy, A.; Beyer, L.; Kolesnikov, A.; Weissenborn, D.; Zhai, X.; Unterthiner, T.; Dehghani, M.; Minderer, M.; Heigold, G.; Gelly, S.; Uszkoreit, J.; and Hounsby, N. 2020. An Image is Worth 16x16 Words: Transformers for Image Recognition at Scale. *International Conference on Learning Representations*.
- Fedus, W.; Zoph, B.; and Shazeer, N. 2022. Switch transformers: Scaling to trillion parameter models with simple and efficient sparsity. *The Journal of Machine Learning Research*, 23(1): 5232–5270.
- Hendrycks, D.; Basart, S.; Mu, N.; Kadavath, S.; Wang, F.; Dorundo, E.; Desai, R.; Zhu, T.; Parajuli, S.; Guo, M.; et al. 2021a. The many faces of robustness: A critical analysis of out-of-distribution generalization. In *IEEE/CVF International Conference on Computer Vision*, 8340–8349.
- Hendrycks, D.; Zhao, K.; Basart, S.; Steinhardt, J.; and Song, D. 2021b. Natural adversarial examples. In *IEEE/CVF Conference on Computer Vision and Pattern Recognition*, 15262–15271.
- Hihn, H.; and Braun, D. A. 2021. Mixture-of-Variational-Experts for Continual Learning. *arXiv:2110.12667*.
- Hwang, C.; Cui, W.; Xiong, Y.; Yang, Z.; Liu, Z.; Hu, H.; Wang, Z.; Salas, R.; Jose, J.; Ram, P.; et al. 2022. Tutel: Adaptive Mixture-of-Experts at Scale. *arXiv:2206.03382*.
- Jacobs, R. A.; Jordan, M. I.; Nowlan, S. J.; and Hinton, G. E. 1991. Adaptive mixtures of local experts. *Neural computation*, 3(1): 79–87.
- Kenton, J. D. M.-W. C.; and Toutanova, L. K. 2019. BERT: Pre-training of deep bidirectional transformers for language understanding. In *NAACL-HLT*, volume 1, 4171–4186.
- Komatsuzaki, A.; Puigcerver, J.; Lee-Thorp, J.; Ruiz, C. R.; Mustafa, B.; Ainslie, J.; Tay, Y.; Dehghani, M.; and Hounsby, N. 2022. Sparse Upcycling: Training Mixture-of-Experts from Dense Checkpoints. *arXiv:2212.05055*.
- Lepikhin, D.; Lee, H.; Xu, Y.; Chen, D.; Firat, O.; Huang, Y.; Krikun, M.; Shazeer, N.; and Chen, Z. 2020. Gshard: Scaling giant models with conditional computation and automatic sharding. *arXiv:2006.16668*.
- Li, B.; Shen, Y.; Yang, J.; Wang, Y.; Ren, J.; Che, T.; Zhang, J.; and Liu, Z. 2022. Sparse Mixture-of-Experts are Domain Generalizable Learners. *arXiv:2206.04046*.
- Liu, Z.; Mao, H.; Wu, C.-Y.; Feichtenhofer, C.; Darrell, T.; and Xie, S. 2022. A convnet for the 2020s. In *IEEE/CVF Conference on Computer Vision and Pattern Recognition*, 11976–11986.
- Lou, Y.; Xue, F.; Zheng, Z.; and You, Y. 2021. Cross-token Modeling with Conditional Computation. *arXiv:2109.02008*.
- Mittal, S.; Bengio, Y.; and Lajoie, G. 2022. Is a modular architecture enough? *Advances in Neural Information Processing Systems*, 35: 28747–28760.
- Mohammed, M.; Liu, H.; and Raffel, C. 2022. Models with Conditional Computation Learn Suboptimal Solutions. In *I Can't Believe It's Not Better Workshop: Understanding Deep Learning Through Empirical Falsification*.
- Mustafa, B.; Riquelme, C.; Puigcerver, J.; Jenatton, R.; and Hounsby, N. 2022. Multimodal contrastive learning with LIMoE: the language-image mixture of experts. *arXiv:2206.02770*.
- Puigcerver, J.; Riquelme, C.; Mustafa, B.; and Hounsby, N. 2023. From sparse to soft mixtures of experts. *arXiv:2308.00951*.
- Recht, B.; Roelofs, R.; Schmidt, L.; and Shankar, V. 2019. Do ImageNet classifiers generalize to ImageNet? In *International Conference on Machine Learning*, 5389–5400.
- Riquelme, C.; Puigcerver, J.; Mustafa, B.; Neumann, M.; Jenatton, R.; Susano Pinto, A.; Keysers, D.; and Hounsby, N. 2021. Scaling vision with sparse mixture of experts. *Advances in Neural Information Processing Systems*, 34: 8583–8595.
- Russakovsky, O.; Deng, J.; Su, H.; Krause, J.; Satheesh, S.; Ma, S.; Huang, Z.; Karpathy, A.; Khosla, A.; Bernstein, M.; Berg, A. C.; and Fei-Fei, L. 2015. ImageNet Large Scale Visual Recognition Challenge. *International Journal of Computer Vision*, 115(3): 211–252.
- Shazeer, N.; Mirhoseini, A.; Maziarz, K.; Davis, A.; Le, Q.; Hinton, G.; and Dean, J. 2017. Outrageously large neural networks: The sparsely-gated mixture-of-experts layer. *arXiv:1701.06538*.
- Strubell, E.; Ganesh, A.; and McCallum, A. 2019. Energy and policy considerations for deep learning in NLP. *arXiv:1906.02243*.
- Tolstikhin, I. O.; Hounsby, N.; Kolesnikov, A.; Beyer, L.; Zhai, X.; Unterthiner, T.; Yung, J.; Steiner, A.; Keysers, D.; Uszkoreit, J.; et al. 2021. Mlp-mixer: An all-mlp architecture for vision. *Advances in neural information processing systems*, 34: 24261–24272.
- Touvron, H.; Cord, M.; Douze, M.; Massa, F.; Sablayrolles, A.; and Jégou, H. 2021. Training data-efficient image transformers & distillation through attention. In *International conference on machine learning*, 10347–10357. PMLR.

Touvron, H.; Cord, M.; and Jégou, H. 2022. Deit III: Revenge of the ViT. In *17th European Conference Computer Vision*, 516–533.

Tu, Z.; Talebi, H.; Zhang, H.; Yang, F.; Milanfar, P.; Bovik, A.; and Li, Y. 2022. Maxvit: Multi-axis vision transformer. In *European Conference on Computer Vision*, 459–479. Springer.

Vaswani, A.; Shazeer, N.; Parmar, N.; Uszkoreit, J.; Jones, L.; Gomez, A. N.; Kaiser, L. u.; and Polosukhin, I. 2017. Attention is All you Need. In Guyon, I.; Luxburg, U. V.; Bengio, S.; Wallach, H.; Fergus, R.; Vishwanathan, S.; and Garnett, R., eds., *Advances in Neural Information Processing Systems*, volume 30.

Wang, H.; Ge, S.; Lipton, Z.; and Xing, E. P. 2019. Learning Robust Global Representations by Penalizing Local Predictive Power. In *Advances in Neural Information Processing Systems*, 10506–10518.

Yu, J.; Wang, Z.; Vasudevan, V.; Yeung, L.; Seyedhosseini, M.; and Wu, Y. 2022. Coca: Contrastive captioners are image-text foundation models. *arXiv:2205.01917*.

Yun, S.; Han, D.; Oh, S. J.; Chun, S.; Choe, J.; and Yoo, Y. 2019. CutMix: Regularization Strategy to Train Strong Classifiers With Localizable Features. In *IEEE/CVF International Conference on Computer Vision*.

Zhai, X.; Kolesnikov, A.; Houlsby, N.; and Beyer, L. 2022. Scaling vision transformers. In *IEEE/CVF Conference on Computer Vision and Pattern Recognition*, 12104–12113.

Zhang, H.; Cisse, M.; Dauphin, Y. N.; and Lopez-Paz, D. 2018. mixup: Beyond Empirical Risk Minimization. In *International Conference on Learning Representations*.

Zhong, Z.; Zheng, L.; Kang, G.; Li, S.; and Yang, Y. 2020. Random Erasing Data Augmentation. *AAAI Conference on Artificial Intelligence*, 34(07): 13001–13008.

Zoph, B.; Bello, I.; Kumar, S.; Du, N.; Huang, Y.; Dean, J.; Shazeer, N.; and Fedus, W. 2022. Designing effective sparse expert models. *arXiv:2202.08906*.

Exploration of routing architectures

We investigated three distinct routing architectures for our study:

- “Conv”: A straightforward 1×1 convolution, similar to a linear gate.
- “Cos”: A gate that utilizes cosine similarity for routing, as detailed in (Chi et al. 2022). It is a two-layer architecture, with one linear layer projecting the features to a lower dimensional space and another performing cosine similarity against some learned latent codes.
- “L2”: This is identical to the “Cos” gate, except that it employs the L2-distance for similarity instead of cosine.

We conducted training on the ImageNet-1K dataset using various small networks, each employing different routing mechanisms as displayed earlier. The results, as shown in Table 10, indicate that the simple convolutional (conv) configuration generally yields slightly better performance in most cases. However, when evaluating these models on out-of-distribution (OOD) datasets, the results are more varied. The inclusion of OOD evaluation is crucial as an effective routing mechanism should ideally facilitate an expert decomposition that generalizes well. . Notably, the MoE models that showed superior performance on ImageNet-1K also displayed enhanced robustness in the OOD evaluations.

ConvNext-S					
Gate	IN-1K	IMV2	IMA	IMR	IMSK
no MoE	82.1	70.8	24.2	47.2	33.8
Conv	82.1	71.0	23.8	46.2	32.7
Cos	81.9	70.6	22.3	45.6	33.0
L2	82.0	71.6	25.0	45.9	32.8
ConvNext-S (<i>iso.</i>)					
Gate	IN-1K	IMV2	IMA	IMR	IMSK
no MoE	79.7	68.6	13.0	46.4	34.0
Conv	80.3	68.8	13.5	46.6	34.4
Cos	79.7	68.4	12.2	45.3	33.0
L2	80.1	68.6	13.3	46.1	34.3
ViT-S					
Gate	IN-1K	IMV2	IMA	IMR	IMSK
no MoE	79.8	69.1	19.8	43.4	29.7
Conv	80.5	69.1	20.3	43.2	29.9
Cos	79.7	67.8	15.9	41.6	29.3
L2	80.2	68.8	19.0	41.9	29.2

Table 10: Performance of MoE-Integrated Models vs Non-MoE Baselines: ablation study on the gating network architecture. MoE layers are placed on the last two even layers.

Routing analysis

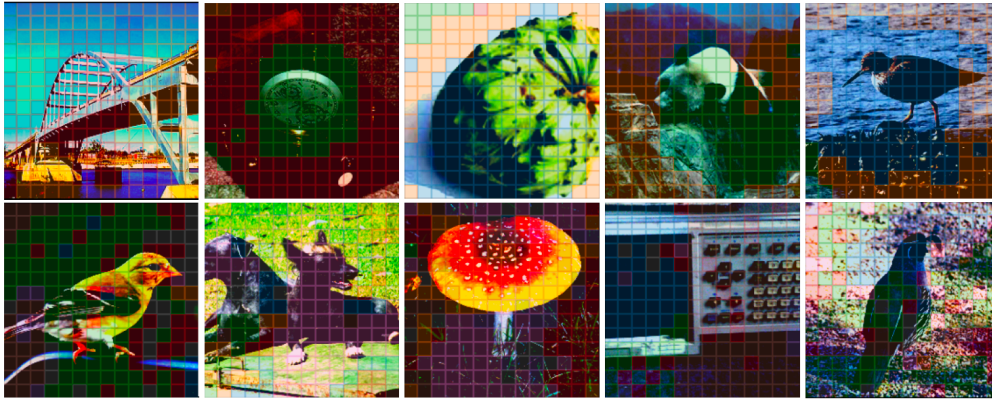


Figure 3: The top row features the ConvNext-T-4 model, while the bottom row showcases the ViT-S-8 model, both of which have been trained on the ImageNet1k dataset. The images displayed have been generated by upsampling the gating output, retaining only the top expert for clarity. Each distinct colour represents a unique expert. These specific images are samples from the ImageNet validation set, extracted from the last third stage of the ConvNext-T-4 and the final layer of the ViT-S-8 models, respectively.

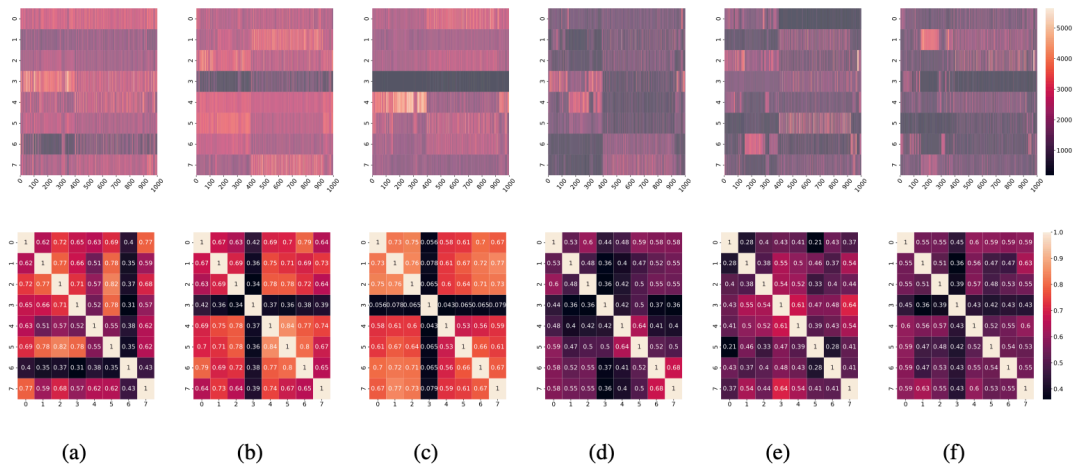


Figure 4: Routing analysis of ViT-S-8, trained on ImageNet-1k. Top row: per-class occurrence of the experts, with the abscissa indicating the class ID and the ordinate representing the expert index (8 experts). Bottom row: similarity score between the experts. The graphs are arranged from left to right from the MoE layer closest to the input (a) to the layer closest to the output (f).

Detailed hyperparameters

Hyperparameter Dataset	ViT (Touvron, Cord, and Jégou 2022)		ConvNext (Liu et al. 2022)	
	IN1k	IN22k	IN1k	IN21k
Batch size	2048	2048	2048	2048
Optimizer	LAMB	LAMB	AdamW	AdamW
LR	$3 \cdot 10^{-3}$	$2.5 \cdot 10^{-3}$	$2.5 \cdot 10^{-3}$	$2.5 \cdot 10^{-3}$
LR decay	cosine	cosine	cosine	cosine
Weight decay	0.03	0.02	0.05	0.05
Expert Weight d.	0.06	0.04	0.05	0.05
Warmup epochs	5	5	20	5
Label smoothing ϵ	0.0	0.1	0.1	0.1
Stoch.Depth	✓	✓	✓	✓
RepeatedAug	✓	✗	✗	✗
H.flip	✓	✓	✓	✓
RRC	✗	✓	✗	✗
Rand Augment	✗	✗	✓	✓
3Augment	✓	✓	✗	✗
Color Jitter	0.3	0.3	✗	✗
Mixup alpha	0.8	0.0	0.8	0.0
Cutmix alpha	1.0	1.0	1.0	1.0
Erasing prob.	✗	✗	0.25	✗
Test crop ratio	1.0	1.0	0.875	0.875
Loss	BCE	CE	CE	CE

Table 11: ImageNet-1k and ImageNet-21k stochastic depth hyperparameter.

Architecture	ImageNet-1k	ImageNet-21k
ViT-(S/B)	0.1 / 0.2	0.0 / 0.1
ConvNext-(T/S/B)	0.1 / 0.3 / 0.6	0.0 / 0.0 / 0.1
ConvNext-(T/B) <i>iso.</i>	0.1 / 0.5	-

Table 12: Summary of our training procedures with ImageNet-1k (IN1k) and ImageNet-21k (IN21k).

Impact of expert size and number

Two critical tunable parameters within the MoE layers are the number of experts per layer and the size of each expert, where size corresponds to the `mlp_ratio`, representing the scaling factor of the hidden layer in the feed-forward network. Figure 5 shows the sensitivity of the results w.r.t. these parameters for ConvNext, with expert counts ranging from 4 to 16 and expert sizes from 1 to 4. Typically, this parameter is preset to 4, implying that using expert sizes less than 4 results in smaller per-sample layers compared to the original network. For comprehensive evaluation, we report the top-1 accuracy for three categories of datasets: independent and identically distributed (i.i.d.) (ImageNet, ImageNetV2 (Recht et al. 2019)), Out of Distribution (o.o.d.) (ImageNet-R (Hendrycks et al. 2021a), ImageNet-SK (Wang et al. 2019)), and adversarial (ImageNet-A (Hendrycks et al. 2021b)). The goal is to ascertain whether a configuration of many smaller experts or fewer larger experts yields superior performance.

Our observations on ConvNext, reveal that while MoE layers may negatively affect performance on o.o.d. datasets, they can maintain or slightly improve performance on i.i.d. datasets. Specifically, when the expert count reaches 16, performance deteriorates across all metrics. On the expert size aspect, smaller experts appear more slightly more resilient to increases in the number of experts. Our results indicate that an optimal configuration tends to involve 4 to 8 experts with a `mlp_ratio` of 2 or 4. Consequently, we adopted a configuration of 4 experts with a `mlp_ratio` of 2 for ImageNet-1K. For the ConvNext isotropic and ViT architecture, reducing the `mlp_ratio` always impairs results and even worst for ViT it produces training instabilities.

On data-augmentation

As shown in the previous section, MoE is sensitive to the amount of data at hand. This sensitivity stems from the inherent structure of MoE, where increasing the number of experts results in each expert operating on a smaller data fraction. Consequently, each expert tends to learn specific data clusters, as discussed by Chen et al. (2022).

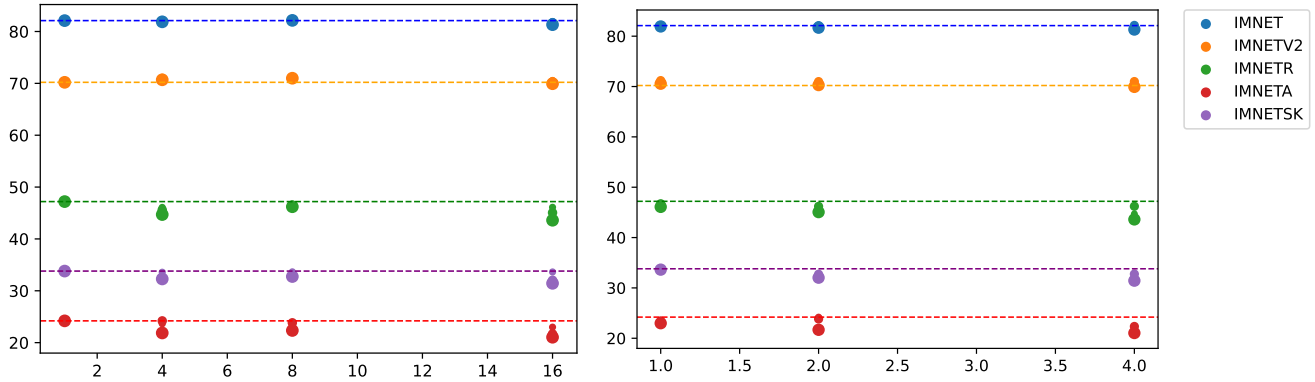


Figure 5: Exploring the interplay between the size and count of experts in a MoE layer for ConvNext-T on ImageNet-1K. Left, x-axis: number of experts. Y-axis: Accuracy on the given test-set. Size of points: MLP-ratio. Right, x-axis: MLP-ratio of experts, i.e., ratio between the number of hidden channels and the number of input/output channels. Y-axis: Accuracy on the given test-set. Size of points: number of experts. Baseline results (without MoE) are denoted by dotted lines. For this small dataset, we observe that MoE does not bring much improvement (see Figure 8 for bigger datasets), the best number of experts is 4 or 8, and the MoE can compensate for the performance loss associated with a smaller model size per sample.

Architecture	# Params ($\times 10^6$)	Per sample #Params _{act}	IN-1K Acc.
ViT-B (Touvron et al. 2021)	86.6	86.6	81.8
ViT-B-8 Every 2 Top 2	284.9	129.9	82.2
ViT-B (Touvron, Cord, and Jégou 2022)	86.6	86.6	82.8
ViT-B-8 Every 2 Top 2	284.9	129.9	82.5

Table 13: ViT-B trained on ImageNet-1k with different hyperparameters. In particular, for the top row (gray) we follow the training recipe from Deit (Touvron et al. 2021) and for the bottom one we follow Deit III (Touvron, Cord, and Jégou 2022).

Modern training methodologies often employ robust data augmentation techniques to enhance model generalization. However, the interplay between these augmentations and the data clusters learned by the MoE model remains relatively uncharted. For instance, techniques like Mixup (Zhang et al. 2018), which blends images, could blur the distinctions between these clusters. Similarly, the Random Resize method, with its aggressive magnification capability, may distort the original data clusters. Understanding the precise influence of these augmentations on the MoE model’s learning process is essential, as it holds implications for the model’s ultimate performance. Some evidence of this can be seen in Table 13. While one training recipe might show MoE outperforming its dense counterparts (as indicated in the top rows of the table), a different, more effective recipe could lead to the opposite outcome (Bottom rows of the table).

More model inspection

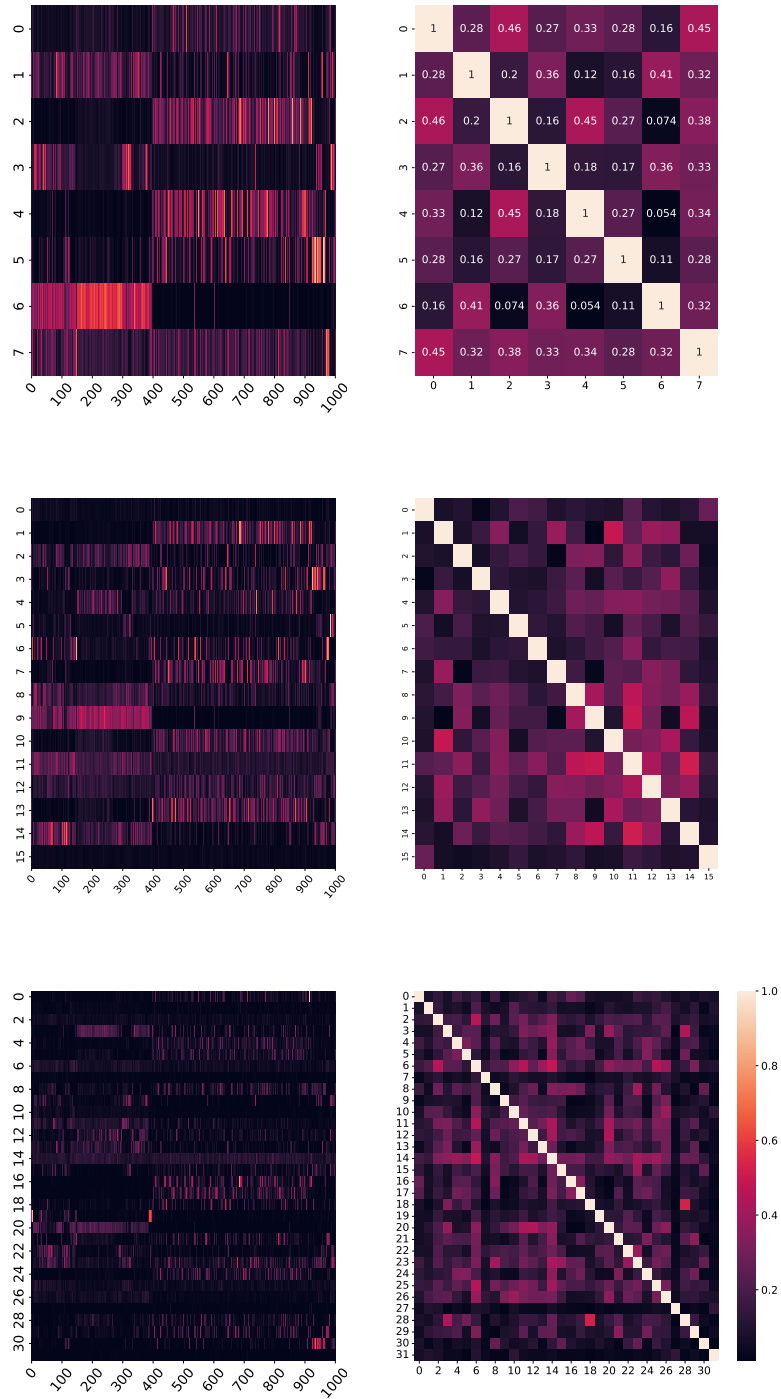


Figure 6: ConvNext-S trained on ImageNet-21k with 8, 16, and 32 experts trained on ImageNet-21k routing analysis. The right columns display the frequency of each expert across different classes, where the x-axis represents class IDs, and the y-axis denotes the expert number. The left column provides a similarity score between experts.

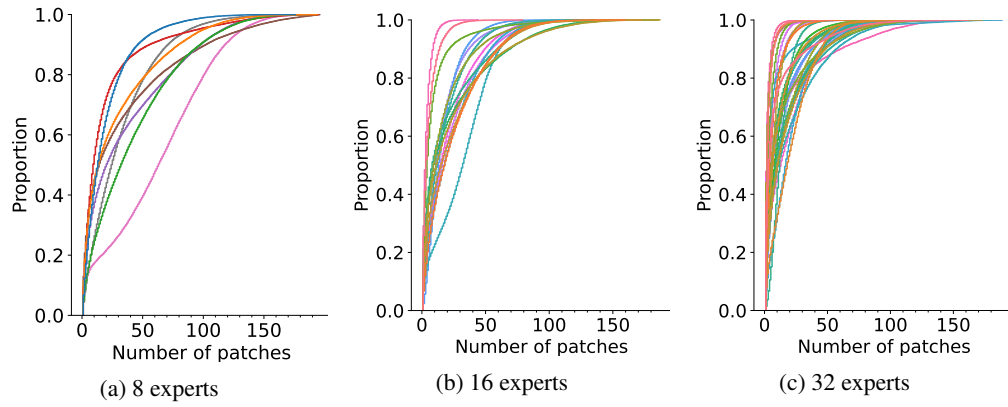


Figure 7: Cumulated Distribution Function of the number of patches used per image for ConvNext-S trained on ImageNet-21k, with 8, 16, and 32 experts. Each colour corresponds to one expert. Sample detailed interpretation: for 8 experts, the “red” expert sees between 1 and 30 patches (out of 196) for 80% of the images on which it is active. In particular (and even more so when there are many experts), an expert frequently covers a limited part of the image. For instance, if the y-axis is close to 1 at x-axis=100 patches, covering more than 100 patches over 196 is rare: experts don’t specialize much. As the number of experts increases, this tendency of experts being used only on a few patches increases too. For 32 experts, most of them focus on less than 30 patches 80% of the time they are active.

MoE vs Dense Table

Architecture	Pre-train dataset	#Params ($\times 10^6$)	Per samples #Params _{act}	IN-1K Acc.
ViT-s/32(Riquelme et al. 2021)	JFT-300M	36.5	36.5	73.73
ViT-s/32-32, Last 2(Riquelme et al. 2021)	JFT-300M	166.7	≈ 55	77.10
ViT-s/32-32, Every 2(Riquelme et al. 2021)	JFT-300M	296.9	≈ 70	77.10
ViT-S/16 (Touvron, Cord, and Jégou 2022)	ImageNet-21k	22.0	22.0	82.6
ViT-S/16-8 Every 2 Top 2	ImageNet-21k	71.7.6	33.1	83.0
ConvNeXt-T (Liu et al. 2022)	ImageNet-21k	28.6	28.6	82.9
ConvNeXt-T-8 Last 2 Top 1	ImageNet-21k	70.0	28.7	83.5
SwinV2-S (Hwang et al. 2022)	ImageNet-21k	65.8	-	83.5
SwinV2-S-8 (Hwang et al. 2022)	ImageNet-21k	173.3	65.8	84.5
SwinV2-S-16 (Hwang et al. 2022)	ImageNet-21k	296.1	65.8	84.9
SwinV2-S-32 (Hwang et al. 2022)	ImageNet-21k	296.1	65.8	84.7
ConvNeXt-S (Liu et al. 2022)	ImageNet-21k	50.3	-	84.6
ConvNeXt-S-8 Last 2 Top 1	ImageNet-21k	91.6	50.3	84.9
ViT-B/16 (Touvron, Cord, and Jégou 2022)	ImageNet-21k	86.6	86.6	85.2
ViT-B/16, Every 2, Top 2	ImageNet-21k	284.9	129.9	85.2
ViT-B/16 \uparrow 384 (Touvron, Cord, and Jégou 2022)	ImageNet-21k	86.6	86.6	86.7
ViT-B/16 (Zhai et al. 2022)	JFT-300M	86.6	86.6	84.9
ViT-B/16 (Riquelme et al. 2021)	JFT-300M	100.5	100.5	84.15
V-MoE-B/16-32, Every 2 (Riquelme et al. 2021)	JFT-300M	979.0	≈ 200	85.3
V-MoE-B/16-32, Last 2 (Riquelme et al. 2021)	JFT-300M	393.3	≈ 110	85.4
SwinV2-B (Hwang et al. 2022)	ImageNet-21k	109.3	109.3	85.1
SwinV2-B-8 (Hwang et al. 2022)	ImageNet-21k	300.3	109.3	85.3
SwinV2-B-16 (Hwang et al. 2022)	ImageNet-21k	518.7	109.3	85.5
SwinV2-B-32 (Hwang et al. 2022)	ImageNet-21k	955.3	109.3	85.5
ConvNeXt-B (Liu et al. 2022)	ImageNet-21k	88.6	88.6	85.8
ConvNeXt-B-8	ImageNet-21k	162.0	88.6	85.7
ViT-L/16 (Touvron, Cord, and Jégou 2022)	ImageNet-21k	304.4	304.4	87.0
ViT-L/16 (Zhai et al. 2022)	JFT-300M	323.1	323.1	87.7
ViT-L/16 (Riquelme et al. 2021)	JFT-300M	323.1	323.1	87.1
V-MoE-L/16-32, Every 2 (Riquelme et al. 2021)	JFT-300M	3446.0	≈ 600	87.4
V-MoE-L/16-32, Last 2 (Riquelme et al. 2021)	JFT-300M	843.6	≈ 380	87.5
SoViT/14(Alabdulmohsin et al. 2023)	JFT-3B	400	400	90.3
ViT-g/14(Zhai et al. 2022)	JFT-3B	1B	1B	90.45
V-MoE/14 (Riquelme et al. 2021)	JFT-3B	15B	$\approx 1B$	90.35

Table 14: Experiments with pretraining on ImageNet-21k, JFT-300M or JFT-3B: performance with/without MoE. In the case of ConvNeXt-T, we get 0.6 improvement, while increasing the number of parameters but almost not the number of per-sample parameters. For ConvNeXt-S, there is a 0.3 improvement. There is an improvement for SwinV2 models, but these were starting lower. Overall, for strong/big models, there is no clear improvements. Results without citations correspond to our work. V-MoE results marked with a star (*) are results taken from their GitHub (tinyurl.com/yb8fze5u). See Figure 2 for an overview. For every model size examined, we present the accuracy metrics obtained after similar numbers of training iterations. Accuracy (Acc.) refers to Top-1 accuracy.

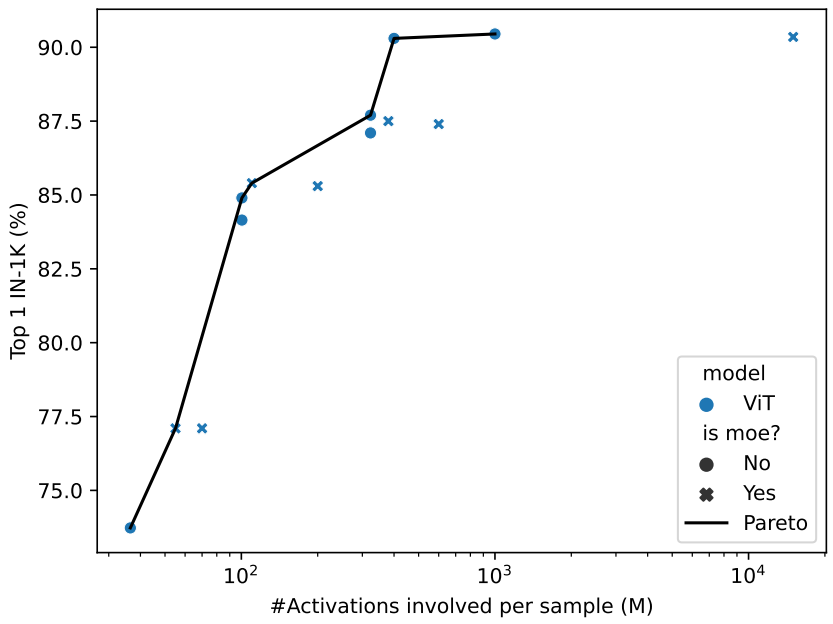
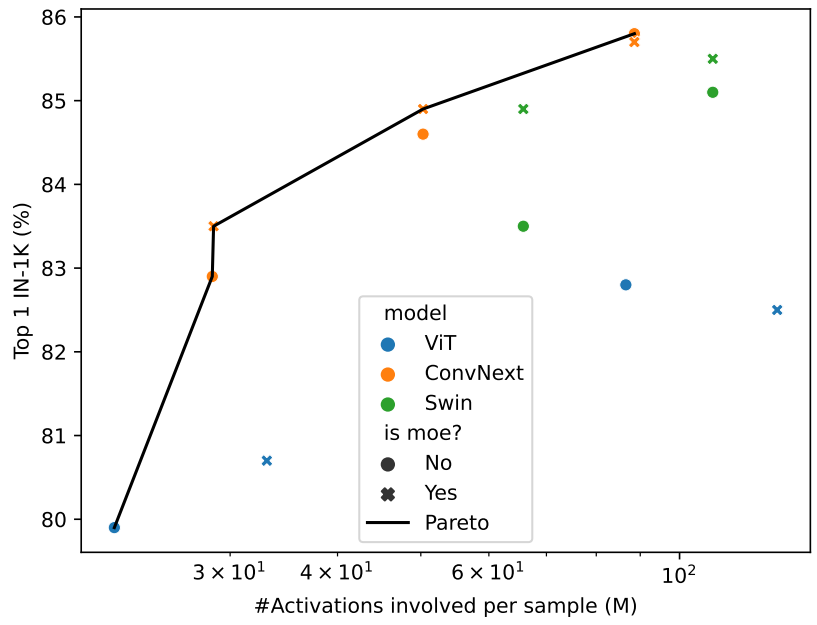


Figure 8: Top: Pareto-front for ImageNet21k, x-axis = number of activations per sample. ViT models have been presented in MoE versions only after additional pretraining, and are therefore not presented. MoE seems to be Pareto optimal for a number of activations per sample below 90M. Bottom: Pareto-front for ViT models on JFT-300M. Overall, MoE is never validated for a number of activations per sample above $\approx 100M$.